Planet Detection Metrics:
Vetting Detection Efficiency

NASA Ames Research Center
Moffett Field, CA 94035

Prepared by: _____ Date: 2015-08-13
Jeffrey L. Coughlin, Kepler Science Office

Approved by: _____ Date: 13 Aug 2015
Natalie Batalha, Kepler Mission Scientist

Approved by: _____ Date: 8/13/15
Michael R. Haas, Kepler Science Office Director

Approved by: _____ Date: 13 Aug '15
Steve B. Howell, Kepler Project Scientist

Document Control

Ownership
This document is part of the Kepler Project Documentation that is controlled by the Kepler Project Office, NASA/Ames Research Center, Moffett Field, California.

Control Level
This document will be controlled under KPO @ Ames Configuration Management system. Changes to this document **shall** be controlled.

Physical Location
The physical location of this document will be in the KPO @ Ames Data Center.

Distribution Requests
To be placed on the distribution list for additional revisions of this document, please address your request to the Kepler Science Office:

> Michael R. Haas
> Kepler Science Office Director
> MS 244-30
> NASA Ames Research Center
> Moffett Field, CA 94035-1000
> Michael.R.Haas@nasa.gov

The correct citation for this document is: J.L. Coughlin 2015, *Planet Detection Metrics: Vetting Detection Efficiency,* KSCI-19096

Contents

1   Introduction

In general, the *Kepler* pipeline generates a list of Threshold Crossing Events (TCEs), which are periodic flux decrements consistent with signals produced by transiting planets. The Threshold Crossing Event Review Team (TCERT) reviews these TCEs, classifying all signals that could possibly be due to astrophysically transiting or eclipsing systems as Kepler Objects of Interest (KOIs). Further review is given to KOIs, such that those conclusively due to eclipsing binaries or contamination from other targets are classified as False Positive (FPs) and the remaining KOIs are classified as Planet Candidates (PCs).

In the first five *Kepler* planet candidate catalogs (Borucki et al., 2011a,b; Batalha et al., 2013; Burke et al., 2014; Rowe et al., 2015) TCERT manually converted interesting TCEs into KOIs, and dispositioned them as PCs and FPs via examination of various plots and quantitative diagnostic tests. In the sixth catalog (Mullally et al., 2015a) TCERT employed partial automation, using simple parameter cuts to automatically cull out a large fraction of TCEs as not transit-like. As well, Mullally et al. (2015a) used an automated technique known as the "centroid robovetter" (Mullally et al., 2015b) to automatically identify some FP KOIs due to centroid offsets — a telltale signature of light contamination from another target. In the latest, seventh catalog (Coughlin et al., 2015a) the entire TCERT process has been automated using what is collectively known simply as "the robovetter".

In order to calculate accurate occurrence rates, the detection efficiency of the *Kepler* pipeline and the TCERT vetting process must be characterized, i.e., how often transiting planets are detected by the pipeline and then classified as planet candidates by TCERT. Christiansen (2015) characterizes the detection efficiency of the *Kepler* pipeline by injecting artificial transits and measuring the number of recovered injected TCEs (injTCEs). This document describes the results of running the robovetter on the recovered injTCEs to determine the TCERT detection efficiency. The results of both exercises are available at the NASA Exoplanet Archive[1].

In §2 we describe the motivation for computing the TCERT detection efficiency and the experimental design. In §3 we describe the table that contains the results of running the robovetter on the injTCEs. Finally, in §4 we show some example products that can be created to assist in the accurate computation of occurrence rates.

2   Experimental Design

As described in Christiansen (2015), the signatures of simulated transiting planets were injected into the Q1–Q17 Data Release 24 (DR24; Thompson et al., 2015) calibrated pixels of ∼200,000 target stars across the focal plane. (Of these injections, ∼159,000 were expected to have at least 3 viable transits, and thus be detectable, given high enough signal-to-noise.) The pixel-level data was then processed through the DR24 version of the *Kepler* pipeline, including data reduction, transiting planet search, and data validation. The simulated transits that were injected had orbital periods ranging from 0.5–500 days and planet radii ranging

---

[1]`exoplanetarchive.ipac.caltech.edu`

from 0.25–7.0 Earth radii. The orbital eccentricities for the injected transits were set to 0, and the impact parameters were drawn from a uniform distribution between 0 and 1. In total, there were 42,264 injTCEs recovered by the pipeline with a similar enough period and epoch compared to the injected period and epoch (Christiansen, 2015). Of these, 6,347 were intentionally injected positionally off-target, i.e., they were injected with a centroid offset. The remaining 35,917 injTCEs were injected at the nominal positions of the target stars.

The set of successfully recovered injTCEs from Christiansen (2015) is an ideal set to determine the TCERT detection efficiency, and is now tractable due to the full automation of the TCERT process by the robovetter. Specifically, it can answer the following questions:

- How often does the robovetter classify an injected planet as a false positive?

- Does the TCERT detection efficiency significantly vary as a function of any parameters, such as signal-to-noise ratio (SNR) or period?

- Which robovetter tests/modules most often fail injected planets, and for what reasons?

To date, it has generally been assumed that the TCERT detection efficiency is very near 100%, i.e., all real planets detected by the pipeline as TCEs are dispositioned as PCs by TCERT. Now, for the first time, we are directly measuring the TCERT detection efficiency as a function of SNR, period, and other parameters of interest for use in occurrence rate calculations. As well, examining the robovetter's behavior on the set of injected planets allows for targeted improvement of the robovetter for the final catalog.

Note that while the injection of on-target transits can tell us how often the robovetter correctly dispositions planetary transit signatures as PCs, it does not tell us how often the robovetter correctly dispositions non-planetary signatures as FPs. The injection of transits with centroid offsets, one type of FP, can be used to determine how often the robovetter correctly identifies that specific type of FP. Simulation of other false positives are being contemplated to characterize the final catalog.

3   Detailed Results Table

We present the parameters that are needed to compute the detection efficiency of the robovetter in the TCERT Detection Efficiency Table, which is hosted at the NASA Exoplanet Archive. This table contains information on every injTCE, i.e., every injected transit signal that was successfully recovered by the *Kepler* pipeline. The table contains 58 columns, which include the robovetter dispositions and major robovetter vetting flags, parameters of the injected signals, parameters from the Data Validation (DV) module of the *Kepler* pipeline, and all TCERT robovetter parameters that were used to disposition each injTCE. Note that in cases where a parameter could not be computed for any reason, it is defaulted to a value of 0.0. In order, these columns are:

- Robovetter Dispositions and Major Flags

    1. Kepler_ID — The *Kepler* ID number of the recovered injTCE.

    2. Disp — The disposition of the recovered injTCE according to the DR24 version of the robovetter (Coughlin et al., 2015a). PC indicates it was dispositioned as a planet candidate, while FP indicates it was dispositioned as a false positive. Note that this disposition and the four major flags below (columns 3–6) are analogous to those shown in the Q1–Q17 DR24 KOI catalog.

    3. NTL — A binary flag indicating whether or not the injTCE was dispositioned as Not Transit-Like (NTL) by the robovetter. A value of "1" indicates it was dispositioned as NTL.

    4. SS — A binary flag indicating whether or not the injTCE was dispositioned as having a Significant Secondary (SS) by the robovetter. A value of "1" indicates it was dispositioned as SS.

    5. CO — A binary flag indicating whether or not the injTCE was dispositioned as having a Centroid Offset (CO) by the robovetter. A value of "1" indicates it was dispositioned as CO.

    6. EM — A binary flag indicating whether or not the injTCE was dispositioned as having an Ephemeris Match (EM) by the robovetter. A value of "1" indicates it was dispositioned as EM.

- Parameters of Injected Transit Signatures

    7. SkyGroup — The sky group of the target star, which identifies the target location by CCD channel for Season 2 (see Appendix D.2 of Thompson & Fraquelli, 2014).

    8. inj_Period — The orbital period in days of the injected signal.

    9. inj_Epoch — The epoch in BKJD (see §6.2.4 of Thompson & Fraquelli, 2014) of the injected signal.

    10. inj_t_depth — The transit depth in ppm of the injected signal.

    11. inj_t_dur — The transit duration in hours of the injected signal.

    12. inj_b — The impact parameter of the injected signal.

    13. inj_Rp/Rs — The ratio of the planet radius to the stellar radius for the injected signal.

    14. inj_a/Rs — The ratio of the semi-major axis of the planetary orbit to the stellar radius for the injected signal.

    15. inj_Offset_flag — A binary flag indicating whether or not the transit was injected with a centroid offset. 0 indicates no centroid offset was injected, while 1 indicates a centroid offset was indeed injected.

    16. inj_Offset_dist — For targets that were injected with a centroid offset, the distance from the target source location to the location of the injected signal, in arcseconds.

17. Expected_MES — The expected Multiple Event Statistic (MES) of the injected signal, which is the *Kepler* pipeline's detection statistic, analogous to SNR.

- DV Parameters

    18. Rp — The radius of the planet in Earth radii as determined by the DV module.

    19. Rs — The radius of the star in solar radii as used by the DV module.

    20. Ts — The temperature of the star in Kelvin as used by the DV module.

    21. a — The semi-major axis of the planet's orbit in AU as determined by the DV module.

    22. Rp/Rs — The radius ratio of the system as determined by the DV module.

    23. a/Rs — The orbital scale of the system as determined by the DV module.

    24. SNR_DV — The SNR of the transit-model fit as determined by the DV module.

    25. Teq — The equilibrium temperature of the planet in Kelvin as determined by the DV module.

    26. Period — The period of the system in days as determined by the DV module.

    27. Epoch — The epoch of the system in BKJD (Thompson & Fraquelli, 2014) as determined by the DV module.

    28. Duration — The duration of the transit in hours as determined by the DV module.

    29. SES_max — The maximum Single Event Statistic (SES) value used in the computation of the injTCE's MES.

    30. MES — The MES of the injTCE, which is the *Kepler* pipeline's detection statistic, analogous to SNR.

- Robovetter Parameters

    - Shape and Odd-Even Metrics

        31. LPP_DV — The LPP transit metric (Thompson, 2015) using the DV detrending. This metric uses the Locality Preserving Projection (LPP) dimensionality reduction algorithm (He & Niyogi, 2004) to identify whether the injTCE is consistent with known transit shapes.

        32. LPP_ALT — The LPP transit metric (Thompson, 2015) using the alternate detrending (Coughlin et al., 2015b).

        33. Marshall — The value of the "Marshall" test (Mullally et al., 2015c) used to identify TCEs due to long-period systematics, such as sudden pixel sensitivity dropouts. Note that this value was only computed for injTCEs with periods greater than 150 days.

        34. σ_oe_dv — The significance of the difference between the odd- and even-numbered primary transits as calculated by the robovetter for the DV detrending.

35. σ_oe_alt — The significance of the difference between the odd- and even-numbered primary transits as calculated by the robovetter for the alternate detrending.

- Model-Shift Test Metrics (Rowe et al., 2015; Coughlin et al., 2015b)

36. σ_pri_dv — The significance of the primary event according to the Model-Shift test using the DV detrending.

37. σ_sec_dv — The significance of the secondary event according to the Model-Shift test using the DV detrending.

38. σ_ter_dv — The significance of the tertiary event according to the Model-Shift test using the DV detrending.

39. σ_pos_dv — The significance of the largest positive event according to the Model-Shift test using the DV detrending.

40. F_red_dv — The ratio of the red noise to the white noise according to the Model-Shift test using the DV detrending.

41. σ_fa_dv — The threshold for an event to be considered statistically significant, and thus not a false alarm (fa), according to the Model-Shift test assuming white noise and using the DV detrending.

42. σ_fa$'$_dv — The threshold for any two events to be considered statistically distinct according to the Model-Shift test assuming white noise and using the DV detrending.

43. σ_pri_alt — The significance of the primary event according to the Model-Shift test using the alternate detrending.

44. σ_sec_alt — The significance of the secondary event according to the Model-Shift test using the alternate detrending.

45. σ_ter_alt — The significance of the tertiary event according to the Model-Shift test using the alternate detrending.

46. σ_pos_alt — The significance of the largest positive event according to the Model-Shift test using the alternate detrending.

47. F_red_alt — The ratio of the red noise to the white noise according to the Model-Shift test using the alternate detrending.

48. σ_fa_alt — The threshold for an event to be considered statistically significant, and thus not a false alarm (fa), according to the Model-Shift test assuming white noise and using the alternate detrending.

49. σ_fa$'$_alt — The threshold for any two events to be considered statistically distinct according to the Model-Shift test assuming white noise and using the alternate detrending.

- Albedo Calculation Metrics

50. Rp — The radius of the planet in Earth radii, calculated by multiplying the radius ratio from the DV module of the *Kepler* pipeline and the stellar radius value from Huber et al. (2014). Note that this value may differ from the value

in column 18 as the DV module utilized stellar parameters that have been updated since Huber et al. (2014).

51. A_dv — The albedo of the planet computed utilizing Model-Shift test metrics from the DV detrending and stellar parameters from Huber et al. (2014).

52. D_pri_dv — The depth of the primary transit calculated by the Model-Shift test on the DV detrending.

53. D_sec_dv — The depth of the secondary eclipse calculated by the Model-Shift test on the DV detrending.

54. Ph_sec_dv — The phase of the secondary eclipse calculated by the Model-Shift test on the DV detrending.

55. A_alt — The albedo of the planet computed utilizing the Model-Shift test metrics from the alternate detrending and the stellar parameters from Huber et al. (2014).

56. D_pri_alt — The depth of the primary transit calculated by the Model-Shift test on the alternate detrending.

57. D_sec_alt — The depth of the secondary eclipse calculated by the Model-Shift test on the alternate detrending.

58. Ph_sec_alt — The phase of the secondary eclipse calculated by the Model-Shift test on the alternate detrending.

- Centroid Metrics

59. Centroid_Bit_Flag — A bit flag to indicate the various reasons the centroid module of the robovetter reached its decision, as detailed in Mullally et al. (2015b). These reasons are combined and stored in a single 32-bit integer, where each bit represents the status of a single flag. We summarize the meaning of each bit below. Of particular interest are Bit 1, which indicates the centroid module recommends that the KOI be marked as FP due to a centroid offset, and Bit 2, which indicates that the robovetter has low confidence in its recommendation. For the Q1–Q17 DR24 KOI catalog a KOI was only marked as a false positive due to centroid offset if the centroid module indicated a high confidence offset, i.e., Bit 1 is set and Bit 2 is not. Bits that are not listed below have internal use only.

   - Bit 1 — The centroid module has decided that the KOI is most likely a false positive due to the transit signal not originating from the target star. Note that if Bit 2 is set the KOI is not marked as FP due to a centroid offset in the robovetter, because of the robovetter's "innocent until proven guilty" philosophy.
   - Bit 2 — The metrics used by the centroid module are very close to the decision boundaries, and thus the centroid disposition of this KOI is uncertain and warrants further scrutiny. In Coughlin et al. (2015a), as well

for the TCERT Detection Efficiency results documented here, no KOIs are marked as FP due to a centroid offset if this bit is set.

- Bit 3 — The centroid module measured the offset distance relative to the star's recorded position in the Kepler Input Catalog (KIC), not the out of transit centroid. The KIC position is less accurate in sparse fields, but more accurate in crowded fields. If this is the only bit set, there is no reason to believe a statistically significant centroid shift is present.

- Bit 4 — Bit 1 was set because there was a statistically significant shift in the centroid during transit.

- Bit 5 — Bit 1 was set because the transit occurs on a star that is spatially resolved from the target.

- Bit 9 — One or more difference images were inverted, meaning the difference image claims the star got brighter during transit. This is usually due to variability of the target star and suggests the difference image should not be trusted. When this bit is set, the KOI is marked as a candidate that requires further scrutiny, i.e., Bit 1 is not set and Bit 2 is set.

- Bit 12 — The star is saturated. The assumptions employed by the centroid module break down for saturated stars, so the KOI is marked as a candidate requiring further scrutiny, i.e., Bit 1 is not set and Bit 2 is set.

- Bit 13 — Fewer than 3 difference images of sufficiently high SNR are available, and thus very few tests are applicable to the KOI. If set in conjunction with Bit 5, the source of the transit may be on a star clearly resolved from the target.

- Bit 14 — The transit was not fit by a model in DV and thus no difference images were created. This bit is typically set for very deep transits due to eclipsing binaries.

- Bit 15 — More than one potential stellar image was found in the difference image. Bit 2 is always set when Bit 15 is set.

- Bit 16 — The PRF fit does not always converge, even in high SNR difference images. This bit is set if centroid offsets are recorded for fewer than 3 high SNR difference images.

- Bit 17 — The uncertainty in the offset significance is high enough that the centroid module can not confidently say whether the significance is above or below the threshold. This bit typically gets set for KOIs with only 3 or 4 recorded centroid measurements.

4   Example Results

In Figure 1 we make plots of the TCERT detection efficiency as a combination of various parameters. We utilize the 35,917 injTCEs without centroid offsets (i.e., using only rows that have the second column, Offset, equal to 0), which is the set of injTCEs that all should be

dispositioned as PC, if the robovetter was perfect. Thus, for each plot in Figure 1, we show the "PC fraction", or the number of injTCEs dispositioned as PC (i.e., the second column, Disp, equal to "PC") in each bin, divided by the total number of injTCEs in each bin.

In general, examining all recovered injTCEs, the robovetter passed 34,210 of the 35,917 injTCEs without centroid offsets, yielding a 95.25% pass rate. Examining Figure 1, specifically the top-left panel, it can be seen that the PC fraction increases with increasing MES. (Note that the *Kepler* pipeline has a minimum detection threshold of 7.1 MES, and very few transit signals were injected with MES greater than 100.) While very low MES detections pass ∼90% of the time, the highest MES detections pass ∼98% of the time, as the vetting metrics become more reliable. Examining the top-right panel, the PC fraction increases with decreasing period. (Note that no signals were injected with periods greater than 500 days.) These two trends can also be seen in the middle-left panel, where the PC fraction is shown as a function of both period and MES, and in the middle-right panel, where the PC fraction is shown as a function of planet radius and period. The bottom-left panel indicates that planets around higher-temperature and more evolved stars may also have decreased PC fractions compared to cooler, main-sequence stars. Finally, as an example for those interested in using this information for occurrence rate calculations, we look at the PC rate of injTCEs with radius (R_p) and insolation flux (S_p) values within 25% of that of Earth's values ($0.75 > \mathrm{R}_p > 1.25\ R_\oplus$ and $0.75 > \mathrm{S}_p > 1.25\ S_\oplus$). There are 118 injTCEs that meet these R_p and S_p criteria, of which 116 are designated planet candidates by the robovetter, therefore yielding a 98.3% PC rate. This can be seen graphically in the bottom-left panel of Figure 1, where the area around Earth's values (1.0, 1.0) shows a very high PC rate. If we add the additional constraint that the host star's effective temperature ($T_\star$) is within 500K of the Sun's, ($5300 < T_\star < 6300$ K), in addition to the previous radius and insolation flux constraints, then the TCERT detection efficiency is 94.5%, as 52 of 55 injTCEs are designated as PCs.

Note that one could make a robovetter with a 100% detection efficiency by simply passing every TCE as a PC — this would be a very poor robovetter though, as it would not identify any false positives. We have specifically designed the robovetter to identify as many false positives as possible while still correctly identifying at least ∼95% of true planetary signals. This means that, in theory, correcting for the robovetter's detection efficiency will only affect derived occurrence rates at the ∼5% level for the entire population, but specific regions may have a lower detection efficiency. As a final reminder, at present (i.e., for DR24) we do not have a measure of how many true, underlying false positives the robovetter dispositions as planet candidates.
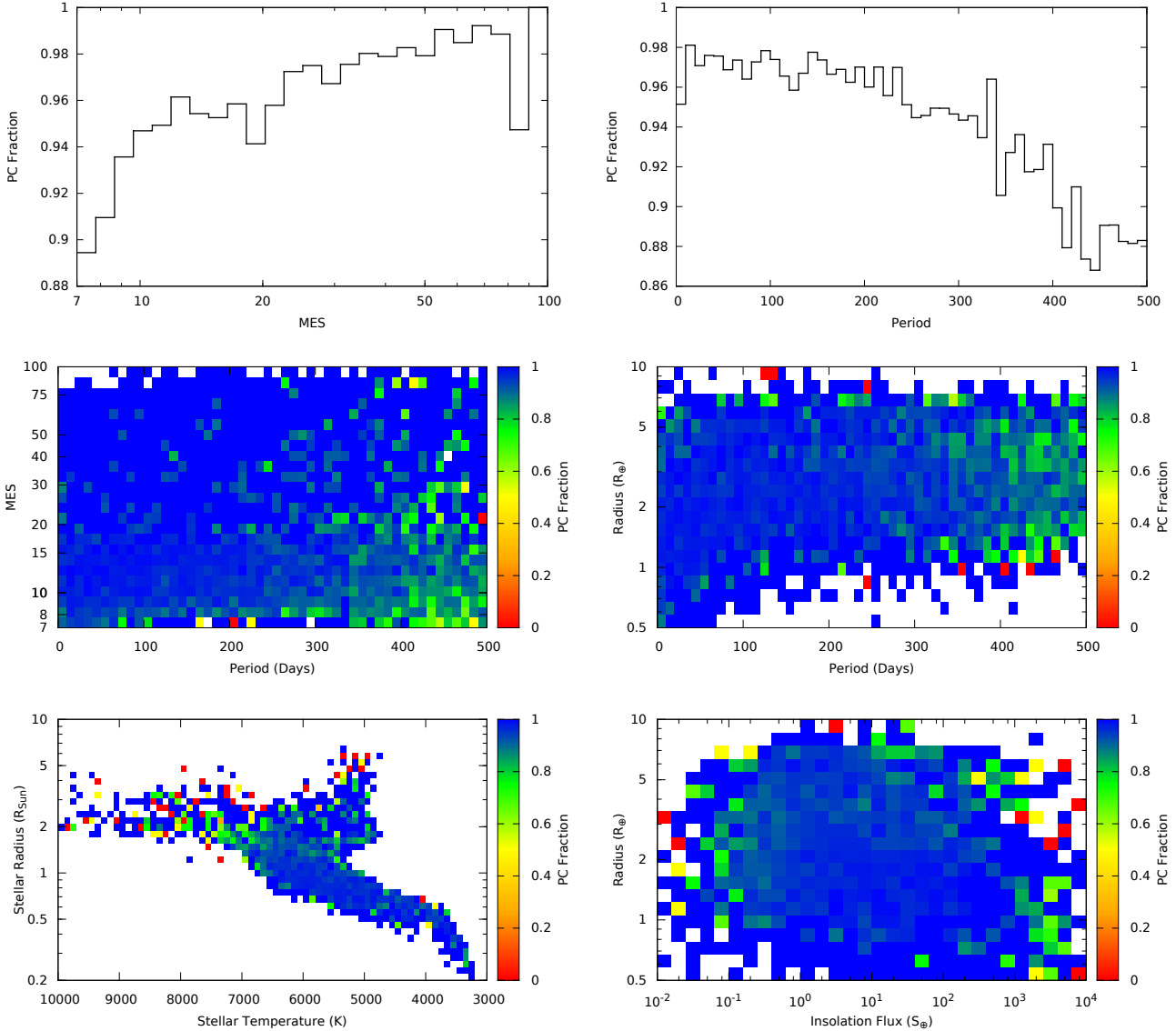
Figure 1: Examples of the TCERT detection efficiency for different combinations of parameters. Top-left: The PC fraction as a function of MES. Top-right: The PC fraction as a function of period. Middle-left: The PC fraction as a function of period and MES. Middle-right: The PC fraction as a function of period and the planet's radius. Bottom-left: The PC fraction as a function of the stellar radius and temperature. Bottom-right: The PC fraction as a function of the planet's radius and insolation flux. Note that the insolation flux was calculated via S = $(T_{eq}/255)^4$, where S is the insolation flux relative to the Earth, T_{eq} is the equilibrium temperature of the planet in Kelvin, and 255K is the Earth's equilibrium temperature.

References

Batalha, N. M., Rowe, J. F., Bryson, S. T., et al. 2013, ApJS, 204, 24

Borucki, W. J., Koch, D. G., Basri, G., et al. 2011a, ApJ, 728, 117

—. 2011b, ApJ, 736, 19

Burke, C. J., Bryson, S. T., Mullally, F., et al. 2014, ApJS, 210, 19

Christiansen, J. L. 2015, Planet Detection Metrics: Pipeline Detection Probability, KSCI-19094-001

Coughlin, J. L., Mullally, F., Thompson, S. E., et al. 2015a, submitted to ApJ

Coughlin, J. L., Bryson, S. T., Burke, C., et al. 2015b, Description of the TCERT Vetting Products for the Q1-Q17 DR24 Catalog (KSCI-19104-001)

He, X., & Niyogi, P. 2004, Advances in Neural Information Processing Systems, 16, 37

Huber, D., Silva Aguirre, V., Matthews, J. M., et al. 2014, ApJS, 211, 2

Mullally, F., Coughlin, J. L., Thompson, S. E., et al. 2015a, ApJS, 217, 31

—. 2015b, submitted to ApJ

—. 2015c, submitted to ApJ

Rowe, J. F., Coughlin, J. L., Antoci, V., et al. 2015, ApJS, 217, 16

Thompson, S. E. 2015, Submitted to ApJ

Thompson, S. E., & Fraquelli, D. 2014, Kepler Archive Manual (KDMC-10008-005)

Thompson, S. E., Jenkins, J. M., Caldwell, D. A., et al. 2015, Kepler Data Release 24 Notes (KSCI-19064-002)